Ground State of Liquid He^4*†

W. P. Francis‡
Department of Physics, University of Windsor, Windsor, Ontario, Canada

and

G. V. Chester
Laboratory of Atomic and Solid State Physics, Cornell University, Ithaca, New York 14850

and

L. Reatto
Istituto di Fisica, Universita di Milano, Milano, Italy

(Received 5 September 1969)

A trial wave function describing the ground state of a quantum system of N interacting bosons is written in the Jastrow form, a product of pair functions. With the interaction potential chosen to represent liquid He^4, and with the parametrized form of the pair function chosen to include a long-range term which has been found necessary to represent the zero-point motion of the long-wavelength density oscillations, a variational calculation has been performed using a new approximate integral equation for the pair distribution function. This equation, which can also be used for classical fluids, is found to be more accurate for repulsive potentials than the Percus-Yevick equation and comparable to (but much simpler than) the Percus-Yevick 2 equation. The essential results are that including the zero-point motion in the wave function tends to lower the energy, raises the equilibrium density, corrects the behavior of the structure function and the momentum distribution of the particles in the low-wave-number region, and slightly decreases the Bose-Einstein condensate fraction. The value of the lower limit on the wavelength of the density oscillations was determined variationally to be about three interparticle spacings.

I. INTRODUCTION

The ground state of liquid He^4(T = 0 °K) has been considered by McMillan[1] and Verlet.[2] The Jastrow form,[3] a product of pair functions, is used as a variational wave function for the quantum system of interacting bosons (He^4 atoms). A parametrized form for the pair function is chosen, and the parameter values are determined by minimizing the ground-state energy. The resulting wave function gave zero-temperature properties of liquid helium generally close to the experimental values.

However, Chester and Reatto[4] have recently revised the form of the pair function to specifically include the zero-point motion of the low-lying long-wavelength phonon modes which are believed to exist in the system. This motion was not present in the wave function used in the calculations of McMillan and Verlet. The phonon effects are particularly dominant in the small-k-region behavior of the structure function $S(k)$ and the momentum distribution of the particles $n(k)$. The present calculation obtains the best wave function and properties of the system by applying the variational principle to the problem, using the form of the pair function suggested by Reatto and Chester.

The long-range nature of the phonon modification introduces a major complication; the previous methods of calculating the two-body correlation function[5] $g(r)$ from the wave function are not feasible. Section II discusses this problem and its resolution, a new approximate integral equation for $g(r)$ called PY2XS. Its mathematical handling is discussed in Appendix A, while its validity is analyzed in Appendix B.

Section III is a presentation of results for the minimum energy per particle, the equilibrium density ρ, the two-body correlation function $g(r)$, the structure function $S(k)$, the Bose-Einstein condensate fraction n_0/ρ, and the momentum distribution $n(k)$. The calculation of the latter two quantities is mathematically analogous to the calculation of the three two-body correlation functions of a two-component mixture system in the low-concentration limit.[6] The PY2XS-mixture integral equations used for this calculation are presented in Appendix C.

II. METHOD OF CALCULATION

Our major task is to calculate the two-body correlation function $g(r)$ from a variational wave function of the form $\prod_{i<j} f(r_{ij})$. The relation between $g(r)$ and $f(r)$ is

$$g(r_{12}) = \Omega^2 \int \cdots \int \prod_{i<j} |f(r_{ij})|^2 \times d3 \cdots dN / \int \cdots \int \prod_{i<j} |f(r_{ij})|^2 d1 \cdots dN , \quad (1)$$

where Ω is the volume of the system and N the number of particles. The formal analogy between this and the classical N-body system at temperature T_{eff}, with pairwise interaction V_C determined by the identification,

$$|f(r)|^2 = e^{-V_c(r)/k_B T_{\text{eff}}} , \qquad (2)$$

allows the use of any of the methods developed in the theory of classical fluids. These methods are called Monte Carlo (MC), molecular dynamics (MD), and approximate integral equations; and they have all been used for the liquid-helium problem.[5]

The pair function suggested by Chester and Reatto is

$$f(r) = \exp\{-\tfrac{1}{2}[(b/r)^m + (uc/\pi^2\rho\hbar)(r^2 + k_c^{-2})^{-1}]\} , \qquad (3)$$

where the second term in the exponent is due to the phonon modes (only phonon modes with wave number in the range $0 \leq k \leq k_c$ are allowed), μ is the He^4 atom mass, and c is the speed of sound in liquid helium. In the absence of the phonon modes, the parameter m was typically 4 or 5.[1,2] So the essential change induced by the second term is to make $\ln f(r)$ long-ranged, i.e., it behaves like r^{-2} instead of r^{-4} or r^{-5} for large r. In fact, it is considered to be of infinite range since it decreases more slowly than r^{-3}.

The long-range character of the new pair function requires a considerably greater range in r space than has previously been used. It is also desirable to obtain $g(r)$ over a larger range to prevent severe truncation error problems in calculating its Fourier transform $S(k)$, especially at low k. The maximum feasible range so far attained by both MC and MD is about $3\sigma(\sigma = 2.556\,\text{Å})$, whereas our problem needs a range of about 10σ. For this reason we are essentially forced to use an approximate integral equation for $g(r)$. The Percus-Yevick (PY1) equation is relatively easy to solve over a 10σ range, but it is a reasonable approximation only for densities less than about $\frac{1}{2}\rho_0$, where $\rho_0 = 2.2 \times 10^{22}$ atoms/cm^3 is the liquid-He^4 equilibrium density. The PY2 equation[7] is reasonably accurate at liquid-helium density, but is sufficiently complicated to make an extension of the range beyond about 3σ impractical.

Our requirements are fulfilled by the new approximate integral equation designated PY2XS. Its accuracy is about that of PY2, while its structure is simple enough to allow a 10σ range even on the CDC 1604 computer available to us, which is considerably slower and smaller than the machines generally used for MC, MD, and PY2.

It is well known that the PY2 equation cannot be considered as a completely systematic extension of the PY1 equation. Indeed, Verlet has proposed two different forms of the PY2 equation. For this reason we see no reason why we should not propose some other form of this equation, particularly if the form we propose is much simpler to compute with and is essentially as accurate as the standard PY2 equation used by Verlet.

The PY2XS equation relates the two-body correlation function $g(r)$, the density ρ, and the product $\beta V(r)$, where $\beta = (k_B T)^{-1}$ and $V(r)$ is the interaction potential. It is convenient to express the equation in terms of the functions,

$$h(r) = g(r) - 1 , \qquad (4)$$

$$Y(r) = g(r)e^{\beta V(r)} - 1 , \qquad (5)$$

and the direct correlation function $C(r)$ defined implicitly by the Ornstein-Zernicke relation,

$$h(r) - C(r) = \rho \int d^3s\, h(|\vec{r} - \vec{s}\,|)C(s) . \qquad (6)$$

The PY2XS equation is then

$$Y(r) = \rho \int d^3s[h(s) - Y(s)]h(|\vec{r} - \vec{s}\,|) + \Phi(r) , \qquad (7)$$

where $$\Phi(0,1) = \tfrac{1}{2}\rho^2 \int\int d2\, d3\, C(0,2)C(0,3) \times g(2,3)\, h(1,2)\, h(1,3), \qquad (8)$$

with vector variables indicated by integers, and $\Phi(r)$ is $\Phi(0,1)$ with $r = |\vec{r}_0 - \vec{r}_1|$. The details of handling the expression for $\Phi(0,1)$ are given in Appendix A.

For a given ρ and $\beta V(r)$, $g(r)$ is obtained by the following double-iteration procedure. The $g(r)$ from the previous outer iteration determines a $C(r)$ by solving Eq. (6) using Fourier transforms. The $\Phi(r)$ is then calculated from these functions and considered a fixed function for the remainder of this outer iteration cycle. The object is now to find the new $g(r)$ which satisfies the PY2XS equation (7) with the $\Phi(r)$ just calculated. This is achieved by an inner iteration loop in which the first term on the right-hand side of Eq. (7) is calculated from the previous (inner) $g(r)$ yielding a new $g(r)$ on the left-hand side. A new $g(r)$ is thus obtained for the next inner iteration. When this inner loop converges, the resultant $g(r)$ is used to begin the next outer cycle. In both the inner and outer loops, an iteration cycle is characterized by an input function and an output function, the function being $\Phi(r)$ for the outer loop and $g(r)$ for the inner loop. The input function for the next iteration is calculated according to the mixing formula

$$F_{\text{in}}^{(i)}(r) = \alpha\, F_{\text{out}}^{(i-1)}(r) + (1-\alpha)\, F_{\text{in}}^{(i-1)}(r), \qquad (9)$$

where $F(r)$ is either $g(r)$ or $\Phi(r)$. Typically the inner loop required 100 iterations with $\alpha = 0.1$, while the outer loop required 10 iterations with $\alpha = 0.8$. $\Phi(r) \equiv 0$ is initially assumed (the PY2XS equation is then just the usual PY1 equation) for the outer loop, whereas $g(r) = e^{-\beta V(r)}$ is the initial assumption for the first inner loop.

III. RESULTS

The pair function $f(r)$, Eq. (3), is uniquely defined by choosing values for the four parameters: b, m, ρ, and k_C. With such a choice the effective $\beta V(r)$ is defined by Eq. (2). This along with ρ then determines a $g(r)$ via the PY2XS equation (7). If the average $\langle F \rangle$ of a function $F(r)$ is defined by

$$\langle F \rangle \equiv \tfrac{1}{2}\rho \int d^3r\, F(r)\, g(r)\,, \tag{10}$$

then the energy per particle $\langle E/N \rangle$ may be expressed as follows[8]:

$$\begin{aligned}
\langle E/N \rangle &= \langle T \rangle + \langle V \rangle\,, \\
\langle V \rangle &= \langle V_1 \rangle + \langle V_2 \rangle\,, \\
\langle V_1 \rangle &= 4\epsilon \langle (\sigma/r)^{12} \rangle\,, \\
\langle V_2 \rangle &= -4\epsilon \langle (\sigma/r)^{6} \rangle\,, \\
\langle T \rangle &= \langle T \rangle_{\mathrm{SR}} + \langle T \rangle_{\mathrm{LR}}\,, \qquad (11) \\
\langle T \rangle_{\mathrm{SR}} &= \frac{\hbar^2}{4\mu\sigma^2} m(m-1)\, b^m \langle (\sigma/r)^{m+2} \rangle\,, \\
\langle T \rangle_{\mathrm{LR}} &= \frac{\hbar^2}{4\mu\sigma^2} \frac{2\sigma}{\rho\sigma^3} \frac{\mu c}{\pi^2\hbar} \left\langle \frac{(r/\sigma)^2 - 3(k_C\sigma)^{-2}}{[(r/\sigma)^2 + (k_C\sigma)^{-2}]^3} \right\rangle, \\
\epsilon &= 10.22\ ^\circ\mathrm{K}\,,
\end{aligned}$$

with the interaction potential of liquid helium being the standard Lennard-Jones potential used by McMillan and Verlet.

In principle, the variational problem may be stated as finding the set of parameter values (b, m, ρ, k_C) giving a minimum $\langle E/N \rangle$. That set would then give the best wave function for the system, at least within the function space spanned by the form, Eq. (3). In practice, the short-range parameters (b, m) are assumed not to change from their best values obtained without the phonon term in the pair function. So we take $b = 1.16$, $m = 5$ to be fixed. It is believed that the effect of this assumption is smaller than that due to the simple form assumed for the pair function, or due to PY2XS being only an approximate equation for $g(r)$, or even due to the uncertainty in the actual interaction potential between two He^4 atoms.[9]

The coupling between the ρ and k_C parameters was found to be weak, so ρ was fixed at ρ_0 for the k_C search. A minimum energy occurred at about $k_C = 0.5\ \text{Å}^{-1}$ which corresponds to a lower bound on the wavelengths of the phonon modes of about three interparticle spacings. It also compares favorably with the upper limit of the phonon portion of the experimental excitation spectrum.

Taking b, m, and k_C to be fixed, the density variation of $\langle E/N \rangle$ is depicted in Fig. 1 for the cases: MD, SR (Verlet)[2]; PY2XS, SR; PY2XS, LR. SR corresponds to $k_C = 0$. The first and second cases directly contrast the effect of the method of solution for $g(r)$, while the second and third cases directly contrast the effect of the phonon modes. Table I lists the minimum energy and equilibrium density for the three cases. One might thereby be tempted to conclude that the effect of the phonon modes is to slightly lower the minimum energy and slightly raise the equilibrium density from the values appropriate to the SR solution. The reality of these effects is jeopardized by the fact that the effects of using PY2XS in place of MD are in the same direction and of the same order of magnitude. However, it does seem reasonable to conclude, at the very least, that including the phonon modes has little effect upon the minimum energy and equilibrium density, and perhaps slightly improves them.

The PY2XS $g(r)$ for $k_C = 0.5\ \text{Å}^{-1}$ (LR) and $\rho = \rho_0$ is given in Table II and plotted in Fig. 2. The

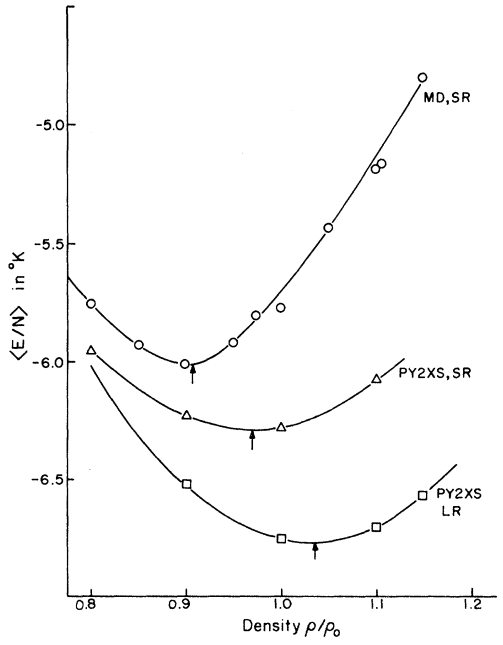

FIG. 1. Variation of energy per particle with density. The system parameters are $m = 5$, $b = 1.16$, and $k_C = 0$ (SR) or $k_C = 0.5\ \text{Å}^{-1}$ (LR). Also, $\rho_0\sigma^3 = 0.3648$ and $\sigma = 2.556$ Å. These system parameters apply to all the figures unless explicitly stated otherwise.

TABLE I. Values of the energy per particle and the density at the variational minimum (see Fig. 1).

	$\langle E/N\rangle_{\min}$ (°K)	ρ_{eq}/ρ_0
MD, SR	−6.015	0.9075
PY2XS, SR	−6.29	0.970
PY2XS, LR	−6.77	1.035

PY2XS, SR $g(r)$ and MD, SR $g(r)$ at the same density are included for contrast. The only marked effect is the general outward shift of the LR $g(r)$ compared to both SR $g(r)$'s as a result of the increased interparticle repulsion from the phonon term. A more interesting contrast is seen in Fig. 3 where the radial probability density for the three cases is shown with the experimentally derived results.[10] The differences among the three theoretical curves are much smaller than the differences between these and the experimental curves. The theoretical curves do not show strong enough correlations for $r/\sigma \geq 2$. This is presumably directly reflected in the main peak discrepancy in $S(k)$ [see Fig. 4] and would seem to be a major failing of the pair function $f(r)$. Its simple form seems to lack the flexibility to accommodate intermediate range correlations, a deficiency apparently unaffected by the phonon term.

The structure function $S(k)$ is defined by

$$S(k) - 1 = \rho \int d^3r\,[g(r) - 1]\,e^{-i\vec{k}\cdot\vec{r}}\,. \qquad (12)$$

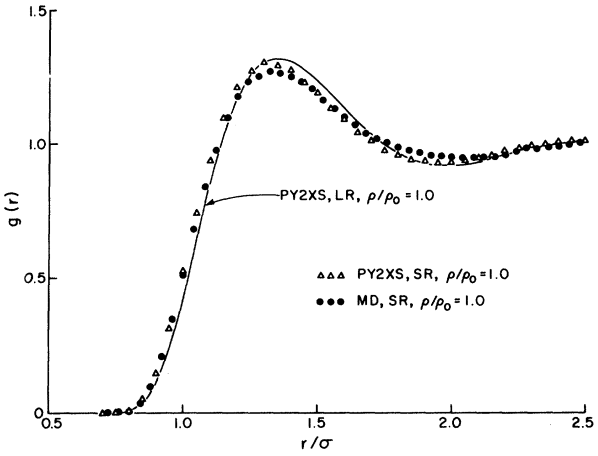

FIG. 2. Pair correlation function $g(r)$.

Table III lists the PY2XS $S(k)$ for $\rho = \rho_0$, $k_c = 0.5\ \text{Å}^{-1}$, while Fig. 4 shows the function as well as the PY2XS, SR functions and the experimental results.[10] Agreement among the results is close except in the main peak region mentioned above ($k\sigma \approx 5$) and in the low-k region, $k\sigma \lesssim 2$. The latter is emphasized in Fig. 5 where the SR and LR PY2XS results, the x-ray data ($T = 1.4$ °K), the theoretical $k \to 0$ limit behavior for a system of phonons at $T = 0$[11]

$$S(k) = \hbar k/2\mu c, \qquad (13)$$

and the Brout formula[12]

TABLE II. Values of the pair correlation function $g(r)$ for $m = 5$, $b = 1.16$, $\rho/\rho_0 = 1.0$, $k_c = 0.5\ \text{Å}^{-1}$.

r/σ	$g(r)$	r/σ	$g(r)$
0.70	0.0000	1.65	1.0791
0.75	0.0007	1.70	1.0432
0.80	0.0073	1.75	0.9967
0.85	0.0375	1.80	0.9729
0.90	0.1158	1.85	0.9434
0.95	0.2540	1.90	0.9338
1.00	0.4423	1.95	0.9208
1.05	0.6504	2.00	0.9235
1.10	0.8555	2.05	0.9239
1.15	1.0257	2.10	0.9340
1.20	1.1634	2.15	0.9426
1.25	1.2479	2.20	0.9562
1.30	1.3044	2.25	0.9686
1.35	1.3116	2.30	0.9817
1.40	1.3103	2.35	0.9938
1.45	1.2714	2.40	1.0037
1.50	1.2383	2.45	1.0132
1.55	1.1796	2.50	1.0191
1.60	1.1380		

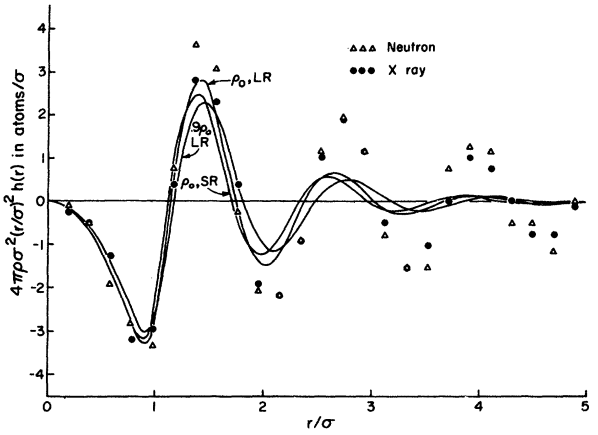

FIG. 3. Radial probability density.

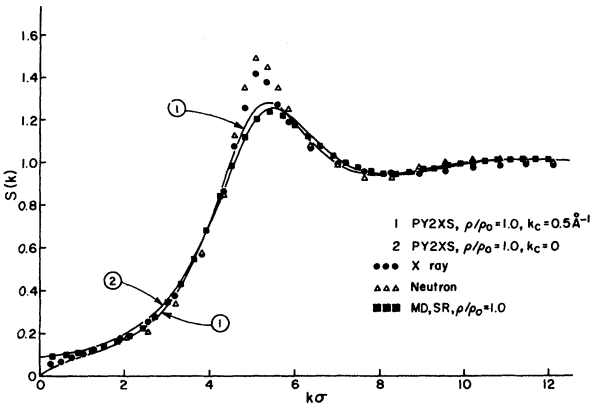

FIG. 4. Structure function $S(k)$.

TABLE III. Values of the structure function $S(k)$ for $m=5$, $b=1.16$, $\rho/\rho_0=1.0$, $k_c=0.5$ Å^{-1}.

$k\sigma$	$S(k)$	$k\sigma$	$S(k)$
0.123	0.0190	4.541	1.0153
0.245	0.0305	4.663	1.0819
0.368	0.0442	4.786	1.1420
0.491	0.0560	4.909	1.1928
0.614	0.0648	5.031	1.2326
0.736	0.0719	5.154	1.2603
0.859	0.0791	5.277	1.2760
0.982	0.0870	5.400	1.2805
1.104	0.0952	5.522	1.2750
1.227	0.1034	5.645	1.2613
1.350	0.1116	5.768	1.2412
1.473	0.1205	5.890	1.2168
1.595	0.1303	6.013	1.1897
1.718	0.1409	6.136	1.1614
1.841	0.1521	6.259	1.1329
1.963	0.1641	6.381	1.1050
2.086	0.1773	6.504	1.078
2.209	0.1920	6.627	1.054
2.332	0.2081	6.995	0.9952
2.454	0.2257	7.118	0.9807
2.577	0.2450	7.240	0.9685
2.700	0.2665	7.383	0.9587
2.823	0.2906	7.486	0.9511
2.945	0.3173	7.609	0.9455
3.068	0.3469	7.731	0.9417
3.191	0.3797	7.854	0.9396
3.313	0.4164	7.977	0.9389
3.436	0.4574	8.468	0.9464
3.559	0.5030	8.958	0.9625
3.682	0.5532	9.449	0.9804
3.804	0.6082	9.940	0.9963
3.927	0.6682	10.431	1.00836
4.050	0.7330	10.922	1.0149
4.172	0.8017	11.413	1.0157
4.295	0.8729	11.904	1.0123
4.418	0.9448	12.395	1.00752

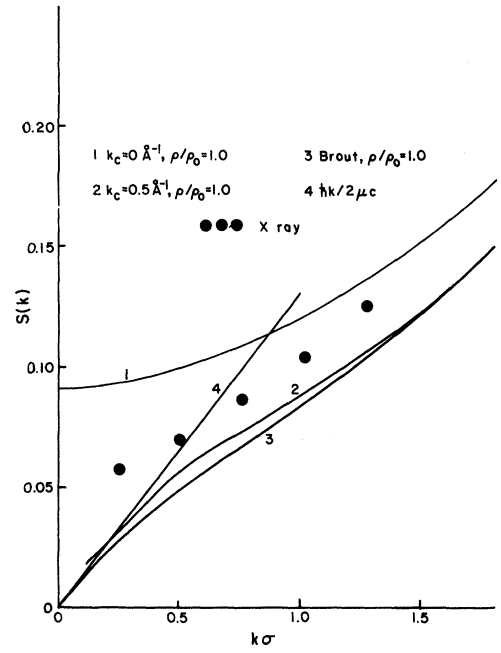

FIG. 5. Behavior of the structure function in the small $k\sigma$ region.

$$S(k;\ k_c) = S(k;\ k_c = 0)/\{1 + (2\mu c/\hbar) \times [\exp(-k/k_c)/k]\ S(k;\ k_c = 0)\} \qquad (14)$$

are displayed. Both the helium system at $T \neq 0$ and any classical fluid exhibit the behavior (χ_T is the isothermal compressibility),[11]

$$S(k) \to \rho\chi_T/\beta + 0(k^2)\ , \quad \text{as } k \to 0\ . \qquad (15)$$

Equation (15) states that $S(k)$ should be quadratic with $S(0) = 0.0506$. The x-ray data fits this behavior well. Equation (15) also explains why the SR $S(k)$ also exhibits quadratic behavior with $S(0) \neq 0$, since the corresponding $g(r)$ is just that for the analogous classical fluid. In sharp contrast to these, the LR $S(k)$ tends to approach the proper linear low-k behavior (the slight upward curvature at $k\sigma \approx 0.2$ is due to truncation errors) even though it was also calculated using the classical system analogy. The infinite-range character of the added phonon term prevents the analogous classical fluid from having a thermodynamic limit which invalidates the argument leading to Eq. (13).[13] The Brout formula has the proper $k \to 0$ limit behavior and is a fair approximation for $k\sigma \lesssim 1.5$, but it does not have the shoulder shown by the PY2XS, LR curve at $k\sigma = 0.5$.

The Bose-Einstein condensate fraction n_0/ρ and the momentum distribution of particles $n(k)$ may be mathematically related to quantities in an equivalent classical system of a two-component mixture of particles.[6] The three interaction potentials for the two-component system are

$$\begin{aligned} \beta V_{11}(r) &= -2\ln f(r)\ , \\ \beta V_{12}(r) &= -\ln f(r)\ , \\ \beta V_{22}(r) &= -\tfrac{1}{2}\ln f(r)\ , \end{aligned} \qquad (16)$$

so the potentials differ only in strength. Subscripts refer to particle species. The densities are $\rho_1 = \rho$ and $\rho_2 \ll \rho_1$ (low-concentration limit). If we define $Y_{22}(r)$ as in Eq. (C4), then we have

$$\rho/n_0 = \lim_{r \to 0}[\ Y_{22}(r) + 1], \qquad (17)$$

$$n(k) = n_0 \int d^3r\, Y_{22}(r) e^{i\vec{k}\cdot\vec{r}}\ . \qquad (18)$$

The function $Y_{22}(r)$ is calculated from the PY2XS mixture equations (presented in detail in Appendix C). Table IV contains the PY2XS result for the condensate fraction and compares it with other values obtained previously. The PY1 entry refers to using the PY1 mixture equations instead of the PY2XS mixture equations. The effect of the zero-point motion of the phonons would seem to be a lowering of the fraction even, perhaps, to the original estimate of Penrose and Onsager.[14]

Figure 6 shows the LR and SR $n(k)$ obtained from PY2XS along with that from McMillan's MC calculations.[1] The primary difference is at low k, where the LR $n(k)$ has the expected k^{-1} behavior,[15] whereas the SR system has a finite $n(k)$, as $k \to 0$.

IV. CONCLUSIONS

Application of the PY2XS integral equation to the LR problem with the short-range parameters $m = 5$, $b = 1.16$ assumed fixed, produced a minimum energy of -6.77 °K at $\rho/\rho_0 = 1.03$ and $k_C = 0.5$ Å^{-1}. The primary conclusion was that in-

TABLE IV. Fraction of particles in the Bose-Einstein condensate. Comparison of values obtained by various methods.

Reference	n_0/ρ, SR	n_0/ρ, LR
McMillan (MC), Ref. 1	0.11 ± 0.01	
Verlet (MD), Ref. 2	0.105 ± 0.005	
PY1, This work	0.25	
PY2XS, This work	0.131	0.101
Penrose and Onsager, Ref. 14	about 0.08	

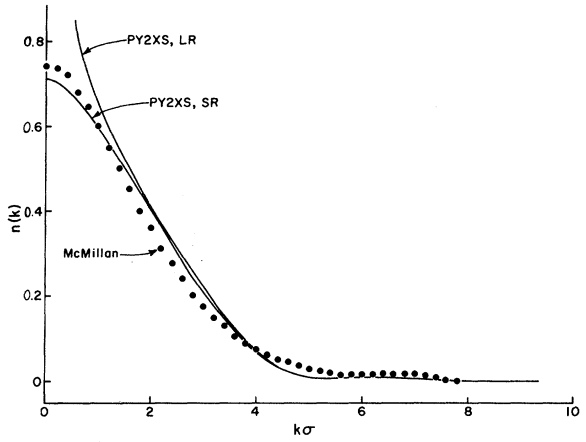

FIG. 6. Momentum distribution function $n(k)$.

cluding the phonons does not change the variational results very much, while the value determined for the phonon-mode wave-number cutoff k_c corresponds to the physically reasonable lower limit on the wavelength of about three interparticle spacings.

The other properties of the ground state did not show striking differences except in the low-k region. The proper linear behavior in $S(k)$ and k^{-1} behavior in $n(k)$ were obtained. The Bose-Einstein condensate fraction was found to be 0.10 with a possible extrapolation to 0.08, taking into account the inherent PY2XS-MD discrepancy. The tendency of the zero-point motion to lower the fraction by about 0.02 did seem to be significant.

This entire set of conclusions rests upon the validity of the PY2XS approximate integral equation. A calculation presently in progress replaces the LR-pair function by an equivalent shorter-range function in the Monte Carlo method. This should present a check on the above conclusions as well as a possible refinement of them.

Note added in proof. If the above conclusions hold also for an interaction potential $V(r)$ with an attractive part, the PY2XS equation would be useful as an accurate and rather simple integral equation for classical fluids at liquid densities. This would be particularly important in the case of liquid metals, where the interaction potential has a rather long tail. This suggests a wider investigation on the limit of validity of the PY2XS equation.

APPENDIX A: MATHEMATICAL HANDLING OF $\Phi(r)$

Care is needed to prevent computer core size and reasonable computation time limits from being exceeded. First we note that the Ornstein-Zernicke equation (6) may be written in the form

$$h(0,1) - C(0,1) = \rho \int d2\, h(0,2)\, C(1,2). \tag{A1}$$

Now writing $g(2,3)$ in terms of $h(2,3)$, Eq. (8) becomes

$$\Phi(0,1) = \tfrac{1}{2}\rho^2 \int\int d2\,d3\, C(0,2)\, C(0,3)\, h(2,3) \times h(1,2)\, h(1,3) + \tfrac{1}{2}\rho^2 \int\int d2\,d3\, C(0,2) \times C(0,3)\, h(1,2)\, h(1,3). \tag{A2}$$

The double integral in the second term factorizes

$$\Phi(0,1) = \text{first term} + \tfrac{1}{2}[\rho \int d2\, C(0,2),\ h(1,2)] \times [\rho \int d3\ C(0,3)\, h(1,3)] \ . \tag{A3}$$

So using (A1), we have

$$\Phi(0,1) = \tfrac{1}{2}\rho^2 \int\int d2\,d3\, C(0,2)\, C(0,3)\, h(2,3) \times h(1,2)\, h(1,3) + \tfrac{1}{2}[h(0,1) - C(0,1)]^2 \ . \tag{A4}$$

Let us proceed to treat the first term. Define

$$I(0,1) = \tfrac{1}{2}\rho^2 \int\int d2\,d3\, C(0,2)\, C(0,3) \times h(2,3)\, h(1,2)\, h(1,3). \tag{A5}$$

Now using the transform for $h(2,3)$ [Eq. (12)], we can effect a factorization of the double integral similar to, but more complicated than, Eq. (A3).

$$I(0,1) = \frac{\rho}{2(2\pi)^3} \int d^3k\, [S(k) - 1] \int d2\, C(0,2) h(1,2) e^{i\vec{k}\cdot\vec{r}_2} \int d3\, C(0,3) h(1,3) e^{-i\vec{k}\cdot\vec{r}_3} \ . \tag{A6}$$

Let us now define

$$H_{\pm\vec{k}}(0,1) \equiv \int d2\, C(0,2)\, h(1,2)\, e^{\pm i\vec{k}\cdot\vec{r}_2} \ . \tag{A7}$$

Choosing $\vec{r}_0 = 0$, this becomes

$$H_{\pm\vec{k}}(\vec{r}_1) = \int d^3r\, C(r)\, h(|\vec{r}_1 - \vec{r}\,|)\, e^{\pm i\vec{k}\cdot\vec{r}}\,. \tag{A8}$$

Choose the coordinate system with z axis coincident with $\vec{r}_1$, and let θ_k be the angle between $\vec{k}$ and z while θ_{kr} designates the angle between $\vec{k}$ and $\vec{r}$. Then, using an expansion in Legendre polynomials, (A8) becomes

$$H_{\pm\vec{k}}(\vec{r}_1) = \int d^3 r C(r)\, h(|\vec{r}_1 - \vec{r}\,|) \sum_{l=0}^{\infty} (2l+1)\, e^{\pm l\pi i/2} j_l(kr)\, P_l(\cos\theta_{kr}), \tag{A9}$$

where $j_l(z)$ is the spherical Bessel function and $P_l(z)$ is the Legendre polynomial. Now the addition theorem for these polynomials gives

$$P_l(\cos\theta_{kr}) = P_l(\cos\theta_k)\, P_l(\cos\theta) + 2 \sum_{m=1}^{l} \frac{(l-m)!}{(l+m)!}\, P_l^{\,m}(\cos\theta_k)\, P_l^{\,m}(\cos\theta)\cos[m(\varphi_k - \varphi)]\,. \tag{A10}$$

When (A10) is used in (A9), the integration over φ will cause all $m > 0$ terms to be zero. So (A9) becomes

$$H_{\pm\vec{k}}(r_1) = 2\pi \sum_{l=0}^{\infty} (2l+1)\, e^{\pm l\pi i/2} P_l(\cos\theta_k) \int_0^{\infty} dr \int_0^{\pi} d\theta\, r^2 C(r)$$

$$\times h\left((r^2 + r_1^{\,2} - 2rr_1\cos\theta)^{1/2}\right) j_l(kr)\sin\theta\, P_l(\cos\theta). \tag{A11}$$

If we now define

$$\psi_l(k, r_1) \equiv \int_0^{\infty} dr\, r^2 j_l(kr)\, C(r) \int_{-1}^{1} dz\, P_l(z)\, h\left((r^2 + r_1^{\,2} - 2rr_1 z)^{1/2}\right), \tag{A12}$$

then we may write (A11) as

$$H_{\pm\vec{k}}(r_1) = 2\pi \sum_{l=0}^{\infty} (2l+1)\, e^{\pm l\pi i/2} P_l(\cos\theta_k)\, \psi_l(k, r_1)\,. \tag{A13}$$

Equations (A8) and (A13) now give for (A6)

$$I(r_1) = \frac{\rho}{4\pi} \int d^3k\,[S(k) - 1] \sum_{l=0}^{\infty} (2l+1) e^{l\pi i/2} P_l(\cos\theta_k)\, \psi_l(k, r_1)\,.$$

$$\times \sum_{l'=0}^{\infty} (2l'+1)\, e^{-l'\pi i/2} P_{l'}(\cos\theta_k)\, \psi_{l'}(k, r_1)\,. \tag{A14}$$

Now the integration over the angles in $\vec{k}$ space gives

$$\int d\Omega_k P_l(\cos\theta_k)\, P_{l'}(\cos\theta_k) = 4\pi\delta_{ll'}/(2l+1). \tag{A15}$$

Thus, we finally have

$$I(r_1) = \rho \sum_{l=0}^{\infty} (2l+1) \int_0^{\infty} dk\, k^2 [S(k) - 1][\psi_l(k, r_1)]^2\,, \tag{A16}$$

along with (A4) and (A5)

$$\Phi(r_1) = I(r_1) + \tfrac{1}{2}[h(r_1) - C(r_1)]^2\,. \tag{A17}$$

Equations (A12), (A16), and (A17) explicitly show how to calculate $\Phi(r)$. Further modifications of (A12) were made for computational advantages. First the spherical Bessel functions $j_l(kr)$ are written in their elementary trigonometric function form wherein each term contains a single $\sin(kr)$ or $\cos(kr)$ factor. This gives the $\psi_l(k, r_1)$ as a sum of terms of the form

$$\int_0^\infty dr\, F(r)\sin(kr)$$

or $$\int_0^\infty dr\, F(r)\cos(kr) \ .$$

The Cooley-Tukey fast Fourier-transform method[16] can then be used for this purpose. Next the integration over z is modified, primarily to eliminate the awkward argument of h. This argument replaces z as the variable of integration, transfers the awkwardness to the Legendre polynomial, and eliminates square roots. Powers of sums of variables (which now appear explicitly in the Legendre polynomial) are expanded using the binomial theorem so that all variables occur only as factors, and hence all but the actual integration variable may be removed from the integral. In this way the integration over z is reduced to moment integrals of h:

$$A_n(x) \equiv \int_0^x dt\, t^n h(t) \ . \tag{A18}$$

These have the useful advantage of being independent of r_1, l, and k, so they need only be recomputed when $h(t)$ changes. Of course, a price has been paid for this; ψ_l has become a sign of many terms. However, this turns out to be a rather good bargain. Performing all the manipulations mentioned, the following form is obtained to replace (A12):

$$\psi_l(k, r_1) = \sum_{n=1}^{l+1} \sum_{n_1} \sum_{s=0}^{n_1} \sum_{s_1=0}^{n_1-s} \beta(l, n, n_1, s, s_1) k^{-n} r_1^{n_1-2s-2s_1-1} I(k, r_1;\ s, 2s_1 - n_1 - n + 1) \ ,$$

$$n_1 = 0, 2, \ldots, l, \text{ for } l \text{ even}; \quad n_1 = 1, 3, \ldots, l, \text{ for } l \text{ odd};$$

$$I(k, r_1;\ i, j) \equiv \int_0^\infty dr\, r^j C(r) [A_{2i+1}(r + r_1) - A_{2i+1}(|r - r_1|)] S(kr),$$

$$S(kr) \equiv \cos(kr), \quad \text{for } j \text{ odd};$$

$$S(kr) \equiv \sin(kr), \quad \text{for } j \text{ even};$$

$$\beta(l, n, n_1, s, s_1) \equiv \frac{(-1)^{s+l+(n-n_1+\epsilon)/2}(l+n_1)![(2l+1)^2 - 1^2]\cdot[(2l+1)^2 - 3^2]\cdots[(2l+1)^2 - (2n-3)^2]}{2^{l+n_1+3n-3}(n-1)!(\frac{1}{2}(l-n_1))!(\frac{1}{2}l+n_1))!\,(n_1-s-s_1)!\,s_1!\,s!}$$

(A19)

(see Table V for values of ϵ).

The largest value required for good numerical accuracy was $l = 3$, while the r-space grid consisted of 20 points per σ over a range of 10σ.

APPENDIX B: VALIDITY OF PY2XS

We wish to establish the validity of the PY2XS approximate integral equation. We do this by comparing results from it with MD calculations which we shall assume to be exact. We shall also compare it to the other approximate integral equations PY1, known to be poor at liquid He^4 density, and PY 2, considered to be fairly good. The most convenient and appropriate test system is the SR, $m = 5$, b = 1.16 pair function. Since $\langle E/N \rangle$ is the important variational quantity, we shall use it as the primary basis for our comparison. But $\langle T \rangle$ (SR only, of course), $\langle V_1 \rangle$, and $\langle V_2 \rangle$ are also interesting since each is directly proportional to an inverse power moment of $g(r)$ [e.g., $\langle T \rangle \propto \int \times d^3r\, r^{-7} g(r)$, see Eq. (11)]. Thus, our test for

TABLE V. Behavior of ϵ for odd and even values of n and l in equation (A19).

n	l	ϵ
odd	odd	0
even	odd	1
even	even	2
odd	even	3

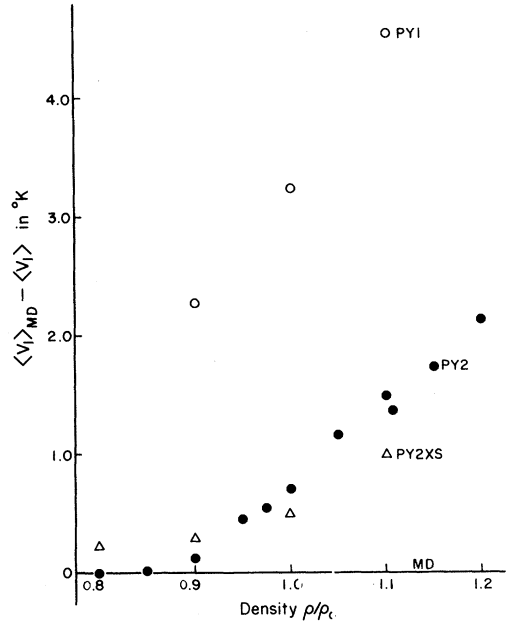

FIG. 7. Comparison of the differences in the values of the inverse 12th moment of $g(r)$ obtained by each integral equation method and molecular dynamics (MD).

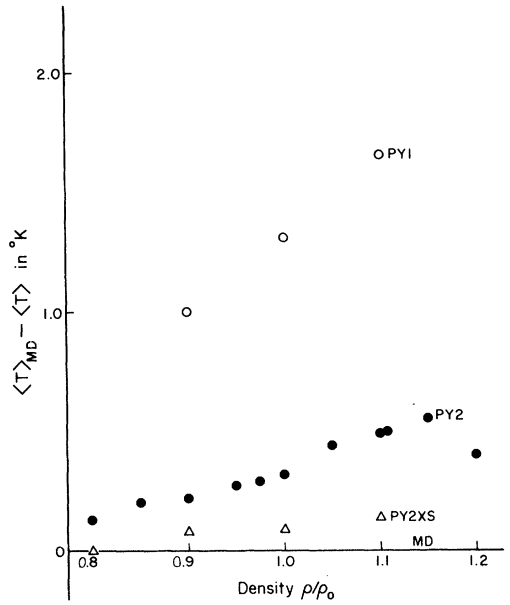

FIG. 9. Inverse seventh moment of $g(r)$ treated as in Fig. 7.

the relative validity of the methods will consist of comparing their results for these averages as a function of density.

Figures 7–9 show the differences between MD and each method's results for $\langle V_1\rangle$, $\langle V_2\rangle$, and $\langle T\rangle$ as a function of density.[17] The following conclusions are apparent. Each method gives poorer results the higher the density. At any fixed density, PY1 is the poorest by far while PY2 and PY2XS are relatively good with PY2XS being slightly better. To give the difference scales a reference, note that at $\rho/\rho_0 = 1.0$, $\langle T\rangle_{MD} = 13.7\,^\circ\mathrm{K}$, $\langle V_1\rangle_{MD} = 17.2\,^\circ\mathrm{K}$, and $\langle V_2\rangle_{MD} = -36.7\,^\circ\mathrm{K}$. Thus, at $\rho/\rho_0 = 1.0$, the relative errors of the PY2XS results compared to MD are about 0.7, 3, and 0.5% in $\langle T\rangle$, $\langle V_1\rangle$, and $\langle V_2\rangle$, respectively. These conclusions are further sup-

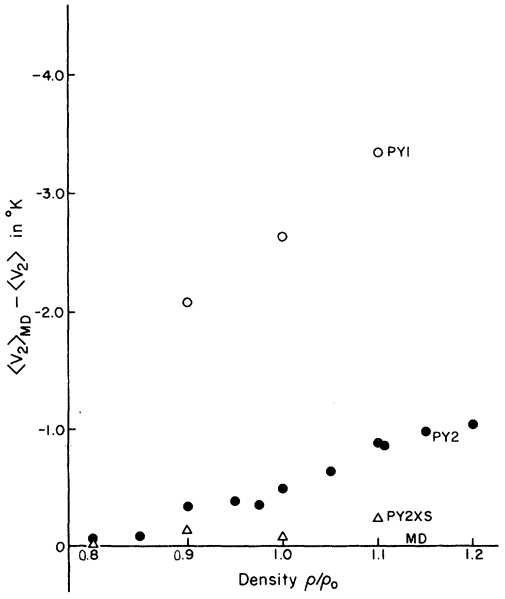

FIG. 8. Inverse sixth moment of $g(r)$ treated as in Fig. 7.

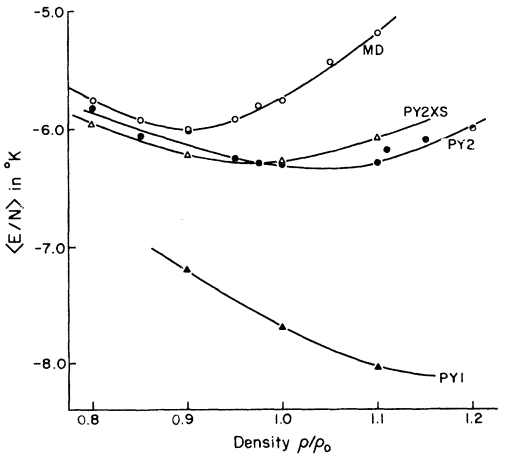

FIG. 10. Method contrast of the variation of the energy per particle as a function of density for the SR system.

ported by the plot of $\langle E/N \rangle$ versus ρ/ρ_0 in Fig. 10. However, the relative error at $\rho/\rho_0 = 1.0$ is now about 8%.

Thus, we are able to conclude that the PY2XS approximate integral equation is somewhat better than PY2 and reasonably close to MD.

APPENDIX C: PY2XS MIXTURE INTEGRAL EQUATIONS

To obtain $Y_{22}(r)$, we modify the PY2 equations for the mixture[18] to get the following PY2XS mixture equations:

$$\Phi_{ij}(1,0) = \tfrac{1}{2} \sum_{k=1}^{2} \sum_{l=1}^{2} \int\int d2\, d3\, \rho_k C_{kj}(2,0) \rho_l C_{lj}(3,0)\, g_{kl}(2,3)\, h_{ik}(1,2)\, h_{il}(1,3), \tag{C1}$$

$$C_{ij}(1,0) = h_{ij}(1,0) - Y_{ij}(1,0) + \Phi_{ij}(1,0), \tag{C2}$$

$$Y_{ij}(1,0) = \Phi_{ij}(1,0) + \sum_{k=1}^{2} \rho_k \int d2 [h_{ik}(1,2) - Y_{ik}(1,2)] h_{kj}(2,0) , \tag{C3}$$

$$Y_{ij}(r) \equiv g_{ij}(r) e^{\beta V_{ij}(r)} - 1 . \tag{C4}$$

For the $\rho_2 \ll \rho_1$ case, (C1) and (C3) simplify to

$$\Phi_{ij}(1,0) = \tfrac{1}{2} \rho_1^2 \iint d2\, d3\, C_{1j}(2,0)\, C_{1j}(3,0)\, g_{11}(2,3) h_{i1}(1,2) h_{i1}(1,3), \tag{C5}$$

$$Y_{ij}(1,0) = \Phi_{ij}(1,0) + \rho_1 \int d2 [h_{i1}(1,2) - Y_{i1}(1,2)] h_{1j}(2,0) . \tag{C6}$$

Thus, we see that

$$Y_{22}(1,0) = \Phi_{22}(1,0) + \rho_1 \int d2 [h_{12}(1,2) - Y_{12}(1,2)] h_{12}(2,0) , \tag{C7}$$

$$\Phi_{22}(1,0) = \tfrac{1}{2} \rho_1^2 \int\int d2\, d3\, C_{12}(2,0)\, C_{12}(3,0)\, g_{11}(2,3) h_{12}(1,2)\, h_{12}(1,3). \tag{C8}$$

So $Y_{22}(r)$ and $\Phi_{22}(r)$ are simply related to the Y_{12} and Φ_{12} functions, which are determined from

$$Y_{12}(1,0) = \Phi_{12}(1,0) + \rho_1 \int d2 [h_{11}(1,2) - Y_{11}(1,2)] h_{12}(2,0), \tag{C9}$$

$$\Phi_{12}(1,0) = \tfrac{1}{2} \rho_1^2 \int\int d2\, d3\, C_{12}(2,0) C_{12}(3,0) g_{11}(2,3) h_{11}(1,2) h_{11}(1,3). \tag{C10}$$

The $i = j = 1$ equations are just the usual PY2XS equations for the pure system [(7) and (8)] due to the decoupling caused by the low-concentration limit, so the Y_{11} and Φ_{11} functions are those already obtained. These are used in (C9) and (C10) which are then solved iteratively [as in solving (7) and (8)] to obtain the Y_{12} and Φ_{12} functions. Equations (C7) and (C8) then produce $Y_{22}(r)$, directly.

†Research was supported in part by the Advanced Research Projects Agency through the Materials Science Center at Cornell University, MSC Report No. 1198, and by the Union Carbide Corporation, and by Comitato Nazionale delle Ricerche.

‡ National Research Council Postdoctorate Fellow.

[1]W. L. McMillan, Phys. Rev. 138, A442 (1965).

[2]D. Schiff and L. Verlet, Phys. Rev. 160, 208 (1967).

[3]R. Jastrow, Phys. Rev. 98, 1479 (1955).

[4]L. Reatto and G. V. Chester, Phys. Rev. 155, 88 (1967).

[5]Reference 2, p. 208.

[6]Reference 4, Sec. V.

[7]L. Verlet, Physica 31, 959 (1965).

[8]Reference 1, Eq. (11).
[9]The last reason can change the ground-state energy by 1 or 2°K. See Ref. 2, p. 212.
[10]For the neutron scattering results, see D. G. Henshaw, Phys. Rev. 119, 9 (1960). For the x-ray scattering, see W. L. Gordon, C. H. Shaw, and J. G. Daunt, J. Phys. Chem. Solids 5, 117 (1958).
[11]See pp. 1202–1203 in R. P. Feynman and M. Cohen, Phys. Rev. 102, 1189 (1956).
[12]See Eq. (3.6) in Ref. 4.
[13]Reference 4, Sec. III.
[14]O. Penrose and L. Onsager, Phys. Rev. 104, 576 (1956).
[15]Reference 4, p. 89.
[16]See, for example, M. L. Forman, J. Opt. Soc. Am. 56, 978 (1966). Of course, the Fourier integral must first be written as a Fourier sum.
[17]The MD results are from Ref. 2, the PY1 and PY2XS results are ours, the PY2 results are from D. Levesque, D. Schiff, K. Tu, and L. Verlet, Laboratoire de Physique Théorique et Hautes Energies, Bâtiment 211, Faculté des Sciences, Orsay (S. & O.) France, Technical Report No. TH. 99, June, 1965 (unpublished).
[18]S. Penn, Physica 39, 17 (1968).

PHYSICAL REVIEW A VOLUME 1, NUMBER 1 JANUARY 1970

Quantum-Mechanical Calculation for the Electron-Impact Broadening of the Resonance Lines of Singly Ionized Magnesium†

O. Bely
Observatoire de Nice, Nice, France
and
Hans R. Griem*
Center for Theoretical Physics, Department of Physics and Astronomy, University of Maryland, College Park, Maryland 20742
(Received 15 August 1969)

Using close-coupling calculations of Burke and Moores for the scattering of electrons by Mg^+ ions in the $3\,^2S_{1/2}$ and $3\,^2P_{1/2,3/2}$ states, Baranger's expression for the impact approximation width of an isolated line is implemented for the components of the resonance doublet. These widths are extrapolated to below inelastic thresholds and averaged over elastic resonances according to theoretical threshold laws. In the experimental energy range, results compare reasonably with semiclassical approximations and with a semiempirical method involving effective Gaunt factors extrapolated to zero electron energy.

I. INTRODUCTION

While semiclassical calculations[1,2] of the broadening of atomic lines by electron impacts are generally in satisfactory agreement with measurements[3] (to about ±20% in terms of widths), ion lines were found to be wider than calculated (assuming straight perturber paths) by factors $\gtrsim 2$ in numerous experiments. However, measured widths were shown in a preceding paper[4] to fit (by factors ~ 1.5 on the average) a semiempirical formula containing effective Gaunt factors, which are only functions of $kT/\Delta E$, i.e., the ratio of perturber (thermal) energy and splitting between levels connected by allowed dipole transitions. These effective Gaunt factors are analogous to those used to estimate inelastic cross sections,[5] but had to be extrapolated[4] below threshold energies to obtain "optical" cross sections in satisfactory agreement with experiment. Presumably this accounted for elastic collisions which would then dominate for $kT/\Delta E \lesssim 1$, a common situation for isolated (not hydrogenic) ion lines. (For atomic lines, the opposite situation $kT/\Delta E > 1$, tends to prevail.)

The importance of elastic contributions had been realized before,[6,7] but their estimations using either a second-order impact parameter method[6,8] (which is, therefore, only first order in the phase shifts, while at least quadratic terms are needed for line widths) or an adiabatic classical-path approximation[7] (which had to be supplemented by semiquantitative criteria to separate inelastic collisions) were almost as *ad hoc* as the effective Gaunt factor method and were much more involved. More-